

# Remote B-Ring Oxidation of Sclareol with an Engineered P450 Facilitates Divergent Access to Complex Terpenoids

Fuzhuo Li,<sup>‡</sup> Heping Deng,<sup>‡</sup> and Hans Renata\*



Cite This: *J. Am. Chem. Soc.* 2022, 144, 7616–7621



Read Online

ACCESS |

Metrics & More

Article Recommendations

Supporting Information

**ABSTRACT:** Though chiral pool synthesis is widely accepted as a powerful strategy in complex molecule synthesis, the effectiveness of the approach is intimately linked to the range of available chiral building blocks and the functional groups they possess. To date, there is still a pressing need for new remote functionalization methods that would allow the installation of useful chemical handles on these building blocks to enable a broader spectrum of synthetic manipulations. Herein, we report the engineering of a  $\text{P}450_{\text{BM}3}$  variant for the regioselective C–H oxidation ofclareol at C6. The synthetic utility of the resulting product was demonstrated in a formal synthesis of ansellone B, the first total synthesis of the 2,3-seco-labdane excolide B, and a model study toward (+)-pallavicinin.

The use of chiral terpene building blocks as starting materials constitutes a powerful approach for the chemical synthesis of complex terpenoid natural products.<sup>1–4</sup> This approach, sometimes referred to as “chiral pool synthesis”, provides several strategic advantages as many of these building blocks are available as single enantiomers at relatively low costs. However, chiral pool synthesis relies heavily on the strategic manipulation of existing functional groups on the building blocks to effect skeletal rearrangements or to rapidly generate structural complexity. A recent review by Maimone and co-workers<sup>4</sup> called for a greater assortment of methodologies to diversify the range of available terpene building blocks and introduce additional chemical handles from which new synthetic disconnections can be made. Though significant effort has been devoted to expanding the synthetic toolbox for the functionalization of chiral terpenes, overriding the innate reactivity profile of these compounds in such functionalization remains challenging.

Motivated by the above limitation, our laboratory has developed an enzymatic C–H oxidation platform for the selective functionalization of drimane-containing building blocks at positions that are previously inaccessible to contemporary chemical methods.<sup>6,7</sup> This approach has proven particularly useful for selective C3 functionalization, which in turn simplified synthetic access to a variety of complex meroterpenoids. Nevertheless, applications of C–H oxidation methodologies on the general drimane skeleton<sup>5</sup> have resulted exclusively in A-ring functionalization and this methodological gap has rendered the chiral pool synthesis of complex terpenoids bearing B-ring oxidation(s) inefficient (Figure 1). To illustrate, Tong and co-workers<sup>8</sup> reported the total synthesis of ansellone B (**1**) via aldehyde **5**. While this intermediate could be converted to **1** in five steps, its preparation fromclareolide (**4**) required 17 steps comprising several indirect functional group manipulations. Though a naturally occurring C6-oxidized labdane diterpene, larisol, has previously been employed in semisynthesis, this compound has

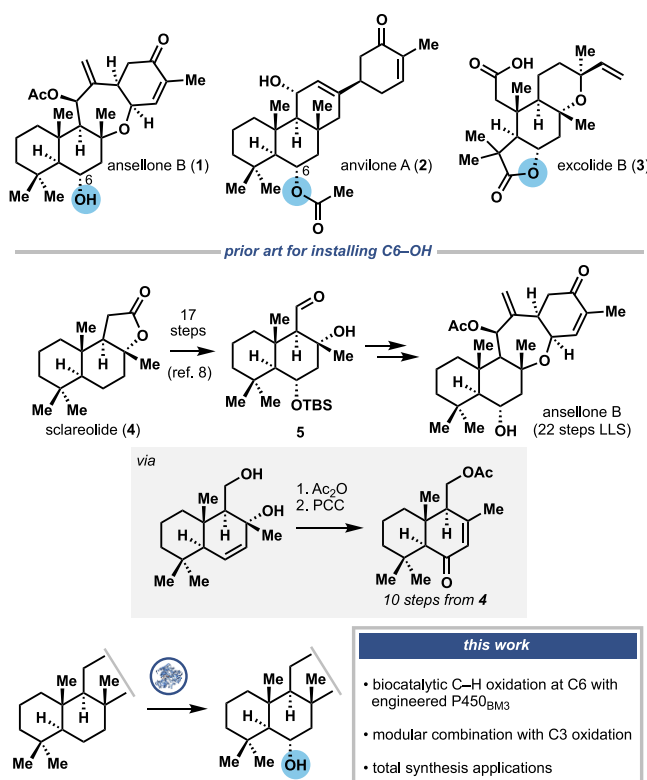
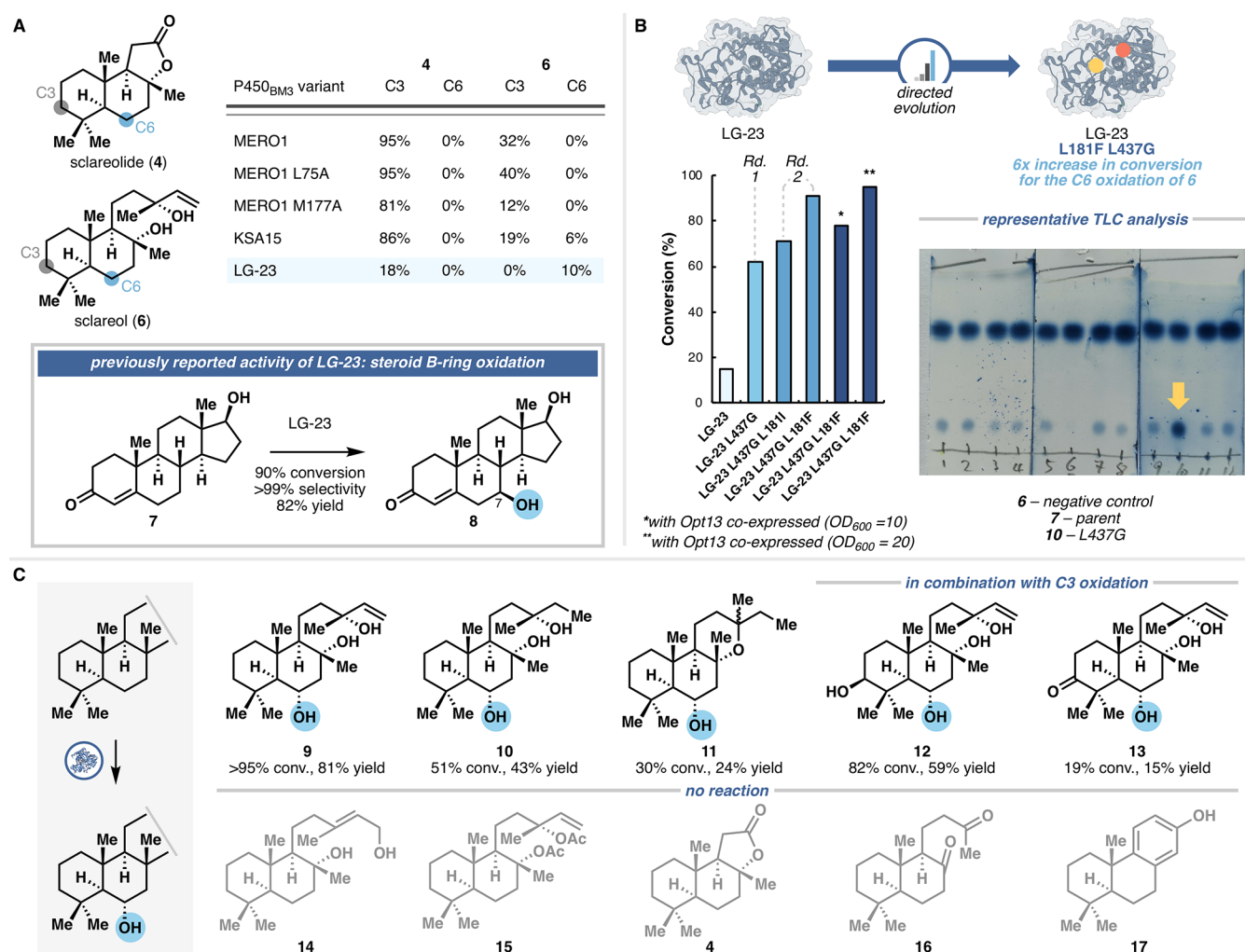


Figure 1. Representative examples of C6-oxidized terpenoids and a lack of efficient method to directly oxidize at C6.

Received: March 18, 2022

Published: April 22, 2022





**Figure 2.** (A) Initial screening of P450<sub>BM3</sub> variants for B-ring oxidation of **4** and **6**. (B) Directed evolution of LG-23 to improve its C6 oxidation activity. Note: Any discrepancies in conversions in Figure 2A and 2B arose because the reactions were performed under different conditions. See Supporting Information for details. (C) Substrate scope for C6 oxidation with LG-23 L181F L437G. Reactions were conducted at 0.1 mmol scale.

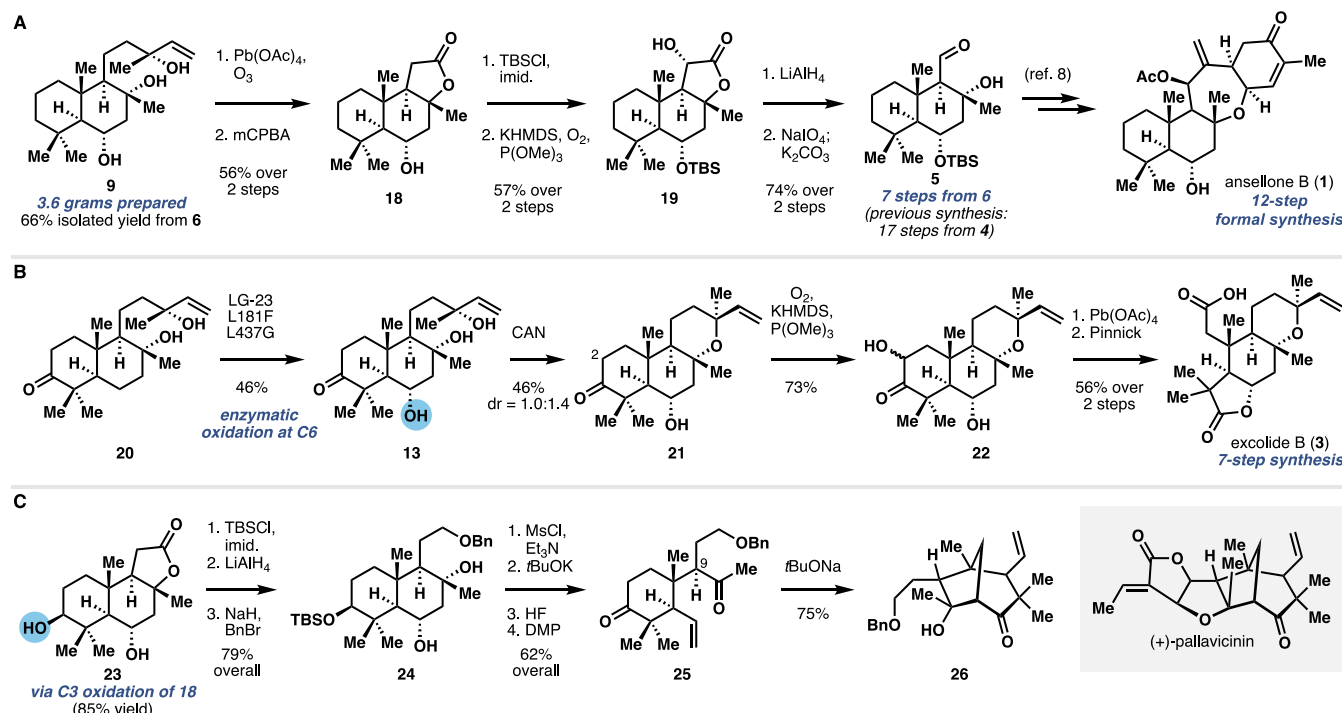
limited commercial availability and needs to be isolated from larix turpentine.<sup>9</sup> In light of these shortcomings, we sought to identify a robust biocatalytic oxidation method to access B-ring oxidized drimanes. This report traces our discovery and engineering of a P450<sub>BM3</sub> variant capable of efficiently catalyzing the C6 oxidation of sclareol and related drimane-containing structures, which subsequently facilitates concise synthetic access to ansellone B (formal synthesis) and excolide B (first total synthesis), and a model study toward pallavicinin. To the best of our knowledge, scalable and site-selective B-ring C–H oxidation of sclareol and related drimanes has not been reported.<sup>10</sup>

We began our work by screening a subset of our library of P450<sub>BM3</sub> variants for the hydroxylation of sclareolide and sclareol (Figure 2A). While progenies of MERO1—a P450<sub>BM3</sub> variant that we previously engineered<sup>6</sup> for the chemoenzymatic synthesis of drimane-containing meroterpenoids—gave exclusively C3 oxidation with both substrates, two variants previously engineered by Reetz and co-workers<sup>11,12</sup> for steroid oxidation (KSA15 and LG-23) afforded C6 oxidation with sclareol. LG-23 in particular delivered exclusively the C6 oxidation product, albeit in low conversion. Notably, this variant was previously engineered for the selective C7 oxidation of testosterone and contains substantially different

active site mutations relative to the MERO1-derived variants and KSA15. LG-23 was next used as a starting point for further mutagenesis. Prior directed evolution of P450<sub>BM3</sub> variants for terpene oxidation has largely relied on a combination of saturation mutagenesis and HPLC or GC analysis.<sup>11–13</sup> For cases that do not permit direct HPLC or GC detection, product derivatizations with chromophoric agents or chromogenic probe substrates are used.<sup>14</sup> As sclareol has a high boiling point and does not possess any chromophore, an alternative screen for direct product detection that does not rely on HPLC or GC was sought. We hypothesized that thin-layer chromatography (TLC) analysis could be adapted for such purpose.<sup>15</sup> Though this screen would not be quantitative, we posited that it would still be sensitive enough to detect big increases in activity. Furthermore, TLC analysis would allow multiple variants to be assayed in parallel in a relatively short time (~5 min/TLC plate containing analytes from 4 different reactions; see Figure 2B), resulting in a comparable, if not superior, throughput to HPLC-based detection.

Following assay development, six active site residues (L75, L78, L82, L181, I263, and L437) in LG-23 were targeted for mutagenesis.<sup>16</sup> As an initial foray, two focused libraries from saturation at L75 and L437 were pursued with the use of the NDT + GCG codon combination. The NDT degenerate

**Scheme 1. (A) Formal Synthesis of Ansellone B from 9; (B) Total Synthesis of Excolide B from 20; (C) Synthesis of (+)-Pallavicin Bicyclic Core from 18**



codon avoids stop codon, encodes for 12 amino acids with a variety of biophysical properties, and has been shown to result in libraries with higher hit rates than NNK libraries.<sup>17</sup> The GCG codon was added to specifically encode for Ala in light of our previous success in identifying beneficial mutations through alanine scanning.<sup>6,7,18</sup> As this design required the screening of 39 clones/site for 95% library coverage, the two saturation libraries could be pursued within a single 96-well plate. Our first round of screening yielded variant LG-23 L437G, which displayed *ca.* 4-fold improvement in the conversion of **6** to **9** upon hit validation while maintaining the exclusive oxidation regioselectivity at C6 (Figure 2B). No beneficial mutation could be identified from the L75X library. LG-23 L437G was used as a parent for the next round of saturation mutagenesis, which targeted residues L181 and I263. Two beneficial mutations, L181I and L181F, were identified from this round. Further hit validation revealed that L181I and L181F mutations conferred 1.2- and 1.5-fold improvement in C6 oxidation activity, respectively. Unfortunately, further mutagenesis of LG-23 L181F L437G by randomizing residues L78 and L82 failed to provide any further improvement. In total, a 6-fold improvement in reaction conversion could be obtained from screening *ca.* 240 clones, showcasing the effectiveness of our directed evolution approach. Preparative scale C6 oxidation of **6** could be performed with lysates of *E. coli* that coexpresses LG-23 L181F L437G and Opt13—an engineered phosphite dehydrogenase<sup>19</sup> for NADPH regeneration through an NADP-dependent oxidation of phosphite to phosphate—to provide >95% conversion and 81% isolated yield of **9**.

With an optimized catalyst in hand, the substrate scope of the reaction was explored (Figure 2C). LG-23 L181F L437G exhibited narrow substrate specificity and high sensitivity to even minor alterations on its substrate structure. For example, the fully reduced counterpart of **6** only displayed 51% reaction

conversion to product **10** and the use of **14**, a constitutional isomer of **6**, completely abolished activity. No reaction could be observed upon capping of the tertiary alcohols of **6** with acetate groups (substrate **15**) either. Interestingly, while the parent enzyme LG-23 showed a low level of C3 oxidation activity on **4**, the double mutant was not able to oxidize this substrate at all, suggesting an activity trade-off during directed evolution. A complete lack of activity was also observed with substrates **16** and **17**. Despite the narrow scope, sclareol derivatives containing additional oxidation at C3 could be accepted in the reaction to provide doubly oxidized products (**12** and **13**) in moderate yields, enabling access to unique building blocks for subsequent synthetic campaigns (*vide infra*).

Docking studies were next pursued to understand the molecular origins of the oxidation regioselectivity and the improved activity during the evolution campaign. Despite our best attempts, a reasonable docking pose for sclareol in the active site of LG-23 could not be obtained. In contrast, a well-defined model could be obtained for the double mutant–sclareol complex (Figure S1). This model shows a notable hydrogen bonding interaction between sclareol's C8-OH with the backbone amide of P329–W330. Mutations L181F and L437G also remodel the active site to provide a suitable hydrophobic pocket to accommodate the pendant prenyl chain of sclareol. These features combine to orient the C6- $\alpha$ H bond toward the heme iron for productive oxidation. In accordance, Type I substrate binding assays revealed a 5-fold decrease in  $K_d$  (2.5  $\mu$ M versus 0.50  $\mu$ M, Figure S2) for the enzyme–sclareol complex after L181F and L437G mutations.

The C6 oxidation products represent versatile synthetic intermediates for the preparation of several complex terpenoids. As noted earlier, aldehyde **5** served as a key intermediate in Tong's synthesis of ansellone B (1),<sup>8</sup> but it had to be prepared from sclareolide in 17 steps. We sought to adapt

several procedures<sup>20</sup> previously described for the conversion of sclareol to sclareolide in the corresponding modification of **9** (Scheme 1A). This effort yielded a two-step sequence featuring oxidative degradation with  $\text{Pb}(\text{OAc})_4$  and  $\text{O}_3$ , followed by an oxidative ring contraction in the presence of mCPBA to afford **18**. TBS protection of the C6 alcohol was followed by a three-step sequence to perform one-carbon excision of the lactone moiety to the corresponding aldehyde (**5**), which intercepts Tong's synthetic route. Overall, this approach constitutes a 12-step formal synthesis of ansellone B and shortens the previous route by 10 steps.

Next, we looked to take advantage of the ability to enzymatically oxidize at C3 and C6 to access the 2,3-*seco*-labdane terpenoid excolide B<sup>21</sup> (Scheme 1B). To this end, ketone **13** was prepared in a three-step sequence from sclareol involving first enzymatic C–H hydroxylation at C3, followed by DMP oxidation and enzymatic C–H hydroxylation at C6. Though **13** was obtained in low conversion in our substrate scope, the enzymatic oxidation conditions could be adjusted by increasing the  $\text{OD}_{600}$  of the cell suspension and decreasing the substrate concentration to provide **13** in 46% isolated yield. Several methods to effect an intramolecular ether ring closure on sclareol have previously been reported.<sup>22</sup> Though the use of  $\text{FSO}_3\text{H}$  provided superior diastereoselectivity to CAN-mediated cyclization, it was found to be incompatible with the free alcohol at C6. For this reason, we elected to move forward with CAN-mediated etherification, even though the desired product was formed only as the minor diastereomer ( $\text{dr} = 1.0:1.4$ ) in the reaction. At this stage, the C2 position of **21** was oxidized via enolate  $\alpha$ -oxidation. Further oxidative cleavage with  $\text{Pb}(\text{OAc})_4$ , followed by Pinnick oxidation completed the first synthesis of excolide B in just 7 steps.

In the same vein, we designed a model study toward the pallavicinin<sup>23</sup> skeleton via a biomimetic Grob fragmentation–aldol cyclization sequence (Scheme 1C). Toward this goal, the C3-OH of **23** was protected as the TBS ether and the resulting product was subjected to reduction with  $\text{LiAlH}_4$ , followed by protection of the resulting primary alcohol to afford intermediate **24**. Mesylation of the C6-OH and treatment of the product with strong base ( $t\text{BuOK}$ ) provided the Grob fragmentation product (S17). During optimization, it was noted that prolonged reaction times would result in the formation of a side product arising from epimerization at C9. Under the best conditions, a diastereomeric ratio of 8:1 favoring the desired product could be achieved. After a two-step conversion of the protected alcohol at C3 to the corresponding ketone, an intramolecular aldol reaction on **25** could be realized in the presence of  $t\text{BuONa}$  to provide the signature bicyclic architecture of (+)-pallavicinin.<sup>24</sup> Once again, precise control of the reaction time was key as an unknown byproduct began to accumulate if the reaction was allowed to proceed for more than 2 h. A key difference between our biomimetic approach and that of Wong and co-workers<sup>25</sup> is the use of an aldehyde motif as the electrophile in the aldol cyclization in the latter, which necessitated additional functional group manipulations to complete the core skeleton of pallavicinin. Our work demonstrates that the correct product diastereomer could be obtained from the methyl ketone precursor, further validating the biosynthetic proposal for this natural product.<sup>26</sup>

In conclusion, we have engineered a P450<sub>BM3</sub> variant capable of catalyzing the C6 oxidation of sclareol and related drimanes and demonstrated the utility of this transformation in the

synthesis of several complex terpenoids. Starting from variant LG-23, two rounds of directed evolution were performed to boost the oxidation activity by 6-fold. Though the resulting double mutant exhibited a narrow substrate scope, it accepted several substrates containing additional oxidation at C3. These insights allowed us to streamline the synthesis of ansellone B by 10 steps in a formal synthesis effort and realize the first synthesis of excolide B in 7 steps. Future work in this area will focus on expanding the substrate scope of the transformation through further enzyme engineering. Based on our biomimetic approach toward pallavicinin, it is anticipated that a more general C6 oxidation platform would enable a divergent and efficient access to an even broader range of *seco*-labdane natural products.<sup>27</sup>

## ASSOCIATED CONTENT

### Supporting Information

The Supporting Information is available free of charge at <https://pubs.acs.org/doi/10.1021/jacs.2c02958>.

Experimental details, analytical data,  $^1\text{H}$  and  $^{13}\text{C}$  NMR data (PDF)

## AUTHOR INFORMATION

### Corresponding Author

Hans Renata – Department of Chemistry, Scripps Florida, Jupiter, Florida 33458, United States;  [orcid.org/0000-0003-2468-2328](https://orcid.org/0000-0003-2468-2328); Email: [hrenata@scripps.edu](mailto:hrenata@scripps.edu)

### Authors

Fuzhuo Li – Department of Chemistry, Scripps Florida, Jupiter, Florida 33458, United States

Heping Deng – Department of Chemistry, Scripps Florida, Jupiter, Florida 33458, United States

Complete contact information is available at: <https://pubs.acs.org/10.1021/jacs.2c02958>

### Author Contributions

<sup>‡</sup>F.L. and H.D. contributed equally.

### Funding

This work is supported by the National Science Foundation CAREER award (H.R. Grant #1945468), the National Institutes of Health Grant S10 OD021550 (for 600 MHz NMR instrumentation), and the Sloan Foundation.

### Notes

The authors declare no competing financial interest.

## ACKNOWLEDGMENTS

We acknowledge funding from the National Science Foundation CAREER award (H.R. Grant #1945468), the National Institutes of Health Grant S10 OD021550 (for 600 MHz NMR instrumentation), and the Alfred P. Sloan Foundation. We thank Dr. Hajeung Park for his assistance in homology modeling and in silico docking. We are grateful to the Shen and Bannister laboratories for access to their reagents and instrumentation.

## ABBREVIATIONS

HPLC, high-performance liquid chromatography; GC, gas chromatography; TLC, thin-layer chromatography; NADPH, dihydronicotinamide adenine dinucleotide phosphate; mCPBA, *meta*-chloroperoxybenzoic acid; DMP, Dess–Martin

Periodinan; CAN, ceric ammonium nitrate; TBS, *tert*-butyldimethylsilyl

## ■ REFERENCES

- (1) Ho, T.-L. Enantioselective Synthesis. *Natural Products from Chiral Terpenes*; Wiley: New York, 1992.
- (2) Money, T.; Wong, M. K. C. The Use of Cyclic Monoterpoids as Enantiopure Starting Materials in Natural Product Synthesis. *Stud. Nat. Prod. Chem.* **1995**, *16*, 123–288.
- (3) Gaich, T.; Mulzer, J. In *Comprehensive Chirality*; Carreira, E. M., Yamamoto, H., Eds.; Elsevier Ltd.: 2012; Vol. 2, pp 163–206.
- (4) Brill, Z. G.; Condakes, M. L.; Ting, C. P.; Maimone, T. J. Navigating the Chiral Pool in the Total Synthesis of Complex Terpene Natural Products. *Chem. Rev.* **2017**, *117*, 11753–11795.
- (5) (a) Zhang, K.; El Damaty, S.; Fasan, R. P450 Fingerprinting Method for Rapid Discovery of Terpene Hydroxylating P450 Catalysts with Diversified Regioselectivity. *J. Am. Chem. Soc.* **2011**, *133*, 3242–3245. (b) Hernandez-Ortega, A.; Vinaixa, M.; Zebec, Z.; Takano, E.; Scrutton, N. S. A Toolbox for Diverse Oxyfunctionalisation of Monoterpene. *Sci. Rep.* **2018**, *8*, 14396. (c) Kawamata, Y.; Yan, M.; Liu, Z.; Bao, D. H.; Chen, J.; Starr, J. T.; Baran, P. S. Scalable, Electrochemical Oxidation of Unactivated C–H Bonds. *J. Am. Chem. Soc.* **2017**, *139*, 7448–7451. (d) Quinn, R. K.; Konst, Z. A.; Michalak, S. E.; Schmidt, Y.; Szklarski, A. R.; Flores, A. R.; Nam, S.; Horne, D. A.; Vanderwal, C. D.; Alexanian, E. J. Site-Selective Aliphatic C–H Chlorination Using N-Chloroamides Enables a Synthesis of Chlorolissoclimide. *J. Am. Chem. Soc.* **2016**, *138*, 696–702. (e) Hung, K.; Condakes, M. L.; Morikawa, T.; Maimone, T. J. Oxidative Entry into the Illucium Sesquiterpenes: Enantiospecific Synthesis of (+)-Pseudoanisatin. *J. Am. Chem. Soc.* **2016**, *138*, 16616–16619. (f) Chen, M. S.; White, M. C. Combined Effects on Selectivity in Fe-Catalyzed Methylenic Oxidation. *Science* **2010**, *327*, 566–571. (g) Fessner, N. D. P450 monooxygenases enable rapid late-stage diversification of natural products via C–H bond activation. *ChemCatChem.* **2019**, *11*, 2226–2242.
- (6) Li, J.; Li, F.; King-Smith, E.; Renata, H. Merging Chemoenzymatic and Radical-Based Retrosynthetic Logic for Rapid and Modular Synthesis of Oxidized Meroterpenoids. *Nat. Chem.* **2020**, *12*, 173–179.
- (7) Li, F.; Renata, H. A Chiral-Pool-Based Strategy to Access *trans*-*syn*-Fused Drimane Meroterpenoids: Chemoenzymatic Total Syntheses of Polysin, N-Acetyl-polyveoline and the Chrodrimanins. *J. Am. Chem. Soc.* **2021**, *143*, 18280–18286.
- (8) Zhang, W.; Yao, H.; Yu, J.; Zhang, Z.; Tong, R. Total Syntheses of Sesterpenoid Ansellones A and B, and Phorbadiolone. *Angew. Chem., Int. Ed.* **2017**, *56*, 4787–4791.
- (9) (a) Lagnel, B. M. F.; Morin, C.; de Groot, A. Synthesis of Drimanes from (+)-Larixol. *Synthesis* **2000**, *2000*, 1907–1916. (b) Ciocarlan, A. (+)-Larixol and Larixyl Acetate: Syntheses, Phytochemical Studies and Biological Activity Assessments. *Chem. J. Mold.* **2021**, *16*, 30–45.
- (10) Though microbiological oxidations have been reported to provide C6 oxidation on sclareol and related compounds, the transformations are low-yielding and nonselective: (a) Aranda, G.; Lallemand, J.-Y.; Hammoumi, A.; Azerad, R. Microbial Hydroxylation of Sclareol by *Mucor plumbeus*. *Tetrahedron Lett.* **1991**, *32*, 1783–1786. (b) Choudhary, M. I.; Musharraf, S. G.; Sami, A.; Atta-ur-Rahman. Microbial Transformation of Sesquiterpenes, (–)-Ambrox® and (+)-Sclareolide. *Helv. Chim. Acta* **2004**, *87*, 2685–2694. (c) Nasib, A.; Musharraf, S. G.; Hussain, S.; Khan, S.; Anjum, S.; Ali, S.; Atta-ur-Rahman; Choudhary, M. I. Biotransformation of (–)-Ambrox by Cell Suspension Cultures of *Actinidia deliciosa*. *J. Nat. Prod.* **2006**, *69*, 957–959. (d) Hanson, J. R.; Truneh, A. The Biotransformation of Ambrox® and Sclareolide by *Cephalosporium-phidicola*. *Phytochemistry* **1996**, *42*, 1021–1023. (e) Cano, A.; Ramírez-Apan, M. T.; Delgado, G. Biotransformation of Sclareolide by Filamentous Fungi: Cytotoxic Evaluations of the Derivatives. *J. Braz. Chem. Soc.* **2011**, *22*, 1177–1182. (f) García-Granados, A.; Jiménez, M. B.; Martínez, A.; Parra, A.; Rivas, F.; Arias, J. M. Chemical-Microbiological Synthesis of *ent*-13-*epi*-Manoyl Oxides with Biological Activities. *Phytochemistry* **1994**, *37*, 741–747. (g) Fraga, B. M.; González, P.; Guillermo, R.; Hernández, M. G. Microbiological Transformation of Manoyl Oxide Derivatives by *Mucor plumbeus*. *J. Nat. Prod.* **1998**, *61*, 1237–1241.
- (11) Kille, S.; Zilly, F. E.; Acevedo, J. P.; Reetz, M. T. Regio- and Stereoselectivity of P450-Catalysed Hydroxylation of Steroids Controlled by Laboratory Evolution. *Nat. Chem.* **2011**, *3*, 738–743.
- (12) Li, A.; Acevedo-Rocha, C. G.; D’Amore, L.; Chen, J.; Peng, Y.; Garcia-Borrás, M.; Gao, C.; Zhu, J.; Rickerby, H.; Osuna, S.; Zhou, J.; Reetz, M. T. Regio- and Stereoselective Steroid Hydroxylation at C7 by Cytochrome P450 Monooxygenase Mutants. *Angew. Chem., Int. Ed.* **2020**, *59*, 12499–12505.
- (13) For representative examples, see: (a) Chen, W.; Fisher, M. J.; Leung, A.; Cao, Y.; Wong, L. L. Oxidative Diversification of Steroids by Nature-Inspired Scanning Glycine Mutagenesis. *ACS Catal.* **2020**, *10*, 8334–8343. (b) Acevedo-Rocha, C. G.; Gamble, C. G.; Lonsdale, R.; Li, A. T.; Nett, N.; Hoebenreich, S.; Lingnau, J. B.; Wirtz, C.; Fares, C.; Hinrichs, H.; Dege, A.; Mulholland, A. J.; Nov, Y.; Leys, D.; McLean, K. J.; Munro, A. W.; Reetz, M. T. P450-catalyzed regio- and diastereoselective steroid hydroxylation: efficient directed evolution enabled by mutability landscaping. *ACS Catal.* **2018**, *8*, 3395–3410. (c) Peng, Y.; Gao, C.; Zhang, Z.; Wu, S.; Zhao, J.; Li, A. A Chemoenzymatic Strategy for the Synthesis of Steroid Drugs Enabled by P450 Monooxygenase-Mediated Steroidal Core Modification. *ACS Catal.* **2022**, *12*, 2907–2914. (d) Le-Huu, P.; Heidt, T.; Claasen, B.; Laschat, S.; Urlacher, V. B. Chemo-, Regio-, and Stereoselective Oxidation of the Monocyclic Diterpenoid  $\beta$ -Cembreneol by P450 BM3. *ACS Catal.* **2015**, *5*, 1772–1780.
- (14) For representative examples, see: (a) Zhang, K.; Shafer, B. M.; Demars, M. D., II; Stern, H. A.; Fasan, R. Controlled Oxidation of Remote  $sp^3$  C–H Bonds in Artemisinin via P450 Catalysts with Fine-Tuned Regio- and Stereoselectivity. *J. Am. Chem. Soc.* **2012**, *134*, 18695–18704. (b) Kolev, J. N.; O’Dwyer, K. M.; Jordan, C. T.; Fasan, R. Discovery of Potent Parthenolide-Based Antileukemic Agents Enabled by Late-Stage P450-Mediated C–H Functionalization. *ACS Chem. Biol.* **2014**, *9*, 164–173. (c) Alwaseem, H.; Giovani, S.; Crotti, M.; Welle, K.; Jordan, C. T.; Ghaemmaghami, S.; Fasan, R. Comprehensive Structure-Activity Profiling of Michelolide and its Targeted Proteome in Leukemia Cells via Probe-Guided Late-Stage C–H Functionalization. *ACS Cent. Sci.* **2021**, *7*, 841–857. (d) de Rond, T.; Gao, J.; Zargar, A.; de Raad, M.; Cunha, J.; Northen, T. R.; Keasling, J. D. A High-Throughput Mass Spectrometric Enzyme Activity Assay Enabling the Discovery of Cytochrome P450 Biocatalysts. *Angew. Chem., Int. Ed.* **2019**, *58*, 10114–10119.
- (15) For several examples of TLC-based assays in directed evolution, see: (a) Zhou, Q.; Hu, M.; Zhang, W.; Jiang, L.; Perrett, S.; Zhou, J.; Wang, J. Probing the Function of the Tyr-Cys Cross-Link in Metalloenzymes by the Genetic Incorporation of 3-Methylthiptyrosine. *Angew. Chem., Int. Ed.* **2013**, *52*, 1203–1207. (b) Liu, X.; Li, J.; Hu, C.; Zhou, Q.; Zhang, W.; Hu, M.; Zhou, J.; Wang, J. Significant Expansion of the Fluorescent Protein Chromophore through the Genetic Incorporation of a Metal-Chelating Unnatural Amino Acid. *Angew. Chem., Int. Ed.* **2013**, *52*, 4805–4809.
- (16) For a comprehensive resource of mutations that have been performed on P450<sub>BM3</sub>, see: Whitehouse, C. J. C.; Bell, S. G.; Wong, L. L. P450<sub>BM3</sub> (CYP102A1): Connecting the Dots. *Chem. Soc. Rev.* **2012**, *41*, 1218–1260. This review suggests that L75, L78, L82, L181, I263, and L437 are common residues to target for mutagenesis in the directed evolution of P450<sub>BM3</sub>.
- (17) (a) Reetz, M. T.; Kahakeaw, D.; Lohmer, R. Addressing the Numbers Problem in Directed Evolution. *ChemBioChem.* **2008**, *9*, 1797–1804. (b) Li, A.; Qu, G.; Sun, Z.; Reetz, M. T. Statistical Analysis of the Benefits of Focused Saturation Mutagenesis in Directed Evolution Based on Reduced Amino Acid Alphabets. *ACS Catal.* **2019**, *9*, 7769–7778.
- (18) Zhang, X.; King-Smith, E.; Dong, L.-B.; Yang, L.-Y.; Rudolf, J. D.; Shen, B.; Renata, H. Divergent Synthesis of Complex Diterpenes through a Hybrid Oxidative Approach. *Science* **2020**, *369*, 799–806.

(19) McLachlan, M. J.; Johannès, T. W.; Zhao, H. Further Improvement of Phosphite Dehydrogenase Thermostability by Saturation Mutagenesis. *Biotechnol. Bioeng.* **2008**, *99*, 268–274.

(20) (a) Alvarez-Manzaneda, E. J.; Chahboun, R.; Alvarez, E.; Fernández, A.; Alvarez-Manzaneda, R.; Haidour, A.; Ramos, J. M.; Akhounz, A. First Enantiospecific Synthesis of Marine Sesquiterpene Quinol Akaol A. *Chem. Commun.* **2012**, *48*, 606–608. (b) Castro, J. M.; Salido, S.; Sánchez, A.; Altarejos, J. Synthesis of (+)-Sclareolide Based on a Cyclic Enol Ether Ring Contraction Induced by Peroxy Acids. *Synlett* **2010**, *2010*, 2747–2750.

(21) Appa Rao Annam, S. CH. V.; Ankireddy, M.; Sura, M. B.; Ponnappalli, M. G.; Sarma, A. V. S.; Jeelani Basha, S. EpimericExcolides from the Stems of *Excoecariaagallocha* and Structural Revision of Rhizophorin A. *Org. Lett.* **2015**, *17*, 2840–2843.

(22) (a) Alvarez-Manzaneda, E. J.; Chaboun, R.; Alvarez, E.; Cabrera, E.; Alvarez-Manzaneda, R.; Haidour, A.; Ramos, J. M. Cerium (IV) Ammonium Nitrate (CAN): A Very Efficient Reagent for the Synthesis of Tertiary Ethers. *Synlett* **2006**, *2006*, 1829–1834. (b) Morarescu, O.; Traistari, M.; Barba, A.; Duca, G.; Ungur, N.; Kulcīki, V. One-Step Selective Synthesis of 13-*epi*-Manoyl Oxide. *Chem. J. Mold.* **2021**, *16*, 99–104.

(23) Chia-Li, W.; Huei-Ju, L.; Huey-Ling, U. A 7,8-Secolabdanoid from the Liverwort *Pallaviciniasubciliata*. *Phytochemistry* **1994**, *35*, 822–824.

(24) An asymmetric synthesis of (−)-pallavicinin has previously been reported by Jia and co-workers: Huang, B.; Guo, L.; Jia, Y. Protecting-Group-Free Enantioselective Synthesis of (−)-Pallavicinin and (+)-Neopallavicinin. *Angew. Chem., Int. Ed.* **2015**, *54*, 13599–13603.

(25) Peng, X.-S.; Wong, H. N. C. Total Synthesis of (±)-Pallavicinin and (±)-Neopallavicinin. *Chem. Asian. J.* **2006**, *1*, 111–120.

(26) Li, Z.-J.; Lou, H.-X.; Yu, W.-T.; Fan, P.-H.; Ren, D.-M.; Ma, B.; Ji, M. Structures and Absolute Configurations of Three 7,8-Secolabdanoid Diterpenes from the Chinese Liverwort *Pallaviciniaambigua*. *Helv. Chim. Acta* **2005**, *88*, 2637–2640.

(27) For a recent review of *secoc*-labdanes and their syntheses, see: Grant, P. S.; Brimble, M. A. *secoc*-Labdanes: A Study of Terpenoid Structural Diversity Resulting from Biosynthetic C–C Bond Cleavage. *Chem.—Eur. J.* **2021**, *27*, 6367–6389.

## □ Recommended by ACS

### Engineered P450 Atom-Transfer Radical Cyclases are Bifunctional Biocatalysts: Reaction Mechanism and Origin of Enantioselectivity

Yue Fu, Peng Liu, *et al.*

JULY 13, 2022

JOURNAL OF THE AMERICAN CHEMICAL SOCIETY

READ 

### Stereoselectivity and Substrate Specificity of the Fe(II)/ $\alpha$ -Ketoglutarate-Dependent Oxygenase TqAL

Hui Tao, Ikuro Abe, *et al.*

NOVEMBER 17, 2022

JOURNAL OF THE AMERICAN CHEMICAL SOCIETY

READ 

### Biocatalytic C14-Hydroxylation on Androstenedione Enabled Modular Synthesis of Cardiotonic Steroids

Yang Zhao, Hui Ming Ge, *et al.*

JULY 28, 2022

ACS CATALYSIS

READ 

### General Synthetic Approach to Diverse Taxane Cores

Melecio A. Perea, Richmond Sarpong, *et al.*

NOVEMBER 08, 2022

JOURNAL OF THE AMERICAN CHEMICAL SOCIETY

READ 

Get More Suggestions >